Transactions of the Nigerian Association of Mathematical Physics
Volume 8, **(***January, 2019***), p145 –152**

MODELLING AND PREDICTION OF TRIBOLOGICAL BALL JOINT FAILUREUNDER FORCED VIBRATION SCENARIO IN AUTOMOBILE SUSPENSION SYSTEMS

I.B. Owunna and A.E. Ikpe

Department of Mechanical Engineering, University of Benin, P.M.B. 1154, Nigeria

Abstract

In vehicles, the ball joint is a very important component that makes up the suspension system, this mechanical component is vital as it is responsible for the vehicle dynamics around curved roads. Due to the condition of our local roads in Nigeria, these components operate under extremely harsh conditions and they tend to fail unexpectedly during service which could be at the detriment of the driver, passengers and other road users. Dimensions of speed bumps and potholes were obtained from the road profile within the University of Benin community through engineered measurement. Employing2017 version of SOLIDWORKS analytical tool, simulation was carried out for static and dynamic conditions with data obtained from the measurement of speed bumps and potholes serving as input forces which were assumed to be acting on the ball joint in real service condition. Considering the yield strength of 620N/mm^2 for EN 18D alloy steel used for the ball joint material, von-mises stress of 377 N/mm^2 and 454 N/mm^2 were obtained from the static and dynamic analysis. Failure was not recorded for both analysis, as the results were in agreement with von-mises failure criterion. Further statistical analysis revealed that the ball joint failure may occur after a period of about 6 months with or without careful driving through Nigerian roads and vice versa. This study has shown that computer based simulation is an effective tool for the prediction of ball joint failure in vehicles prior to occurrence, and can help mitigate against road accident resulting from ball joint failure.

Keywords: Ball Joint, Failure, Prediction, Automobile, Vibration, Road profile.

1. Introduction

Ball joints are widely used in automotive systems such as the suspension and steering linkages and also have its application in human hip joint [1]. Automobile ball joint is a pivoting mechanical element that allows free rotational motion between the wheels of a vehicle and its suspension system. In other words, it is a spherical bearing that connect the control arms to the steering knuckles. The ball joint is one moveable part of a control arm assembly. It is steel bearing stud and socket enclosed in a steel casing [2, 3]. The socket enclosed in steel casing is connected to the control arm. The bearing stud is tapered and threaded so that it fits into a tapered hole in the steering knuckle and the latter connects the tyre [4, 5]. They are used to move front wheel up and down, rotate when steering and change of position and orientation, they transfer the wheel forces without implementing any torque. The joint needs to be free from play but have low internal friction[6]. A standard conventional ball joint has three degrees of freedom and work similarly to the ball-and-socket design of the human hipball. Not only do these ball joints allow the rotations of the steering arms but also perform several other operations in a car sequence to it degree of freedom and connection [7, 8].

The degree of freedom in a ball joint allows the translation of motion in vertical, horizontal and rear axis to the control arms of the steering to enable its rotation. The link between the ball joint, control arm and the steering knuckle is required for the

Correspondence Author: Owunna I.B., Email: ikechukwu.owunna@uniben.edu, Tel: +2349034983495

steering control to rotate horizontally and vertically for shock absorption [9]. The ball joint manufacturing includes a shape designed to the injection mould of the ball seat which is made up of a synthetic resin material that surrounds the outside of the spherical head of the ball stud. A lower mould is installed underneath the upper mould which has a mould surface capable of forming a part of the ball seat; a jig is installed to fix the ball stud in the moulding position of the upper mould and lower mould, and a rotating system is set in place to rotate the fixing jig. This process of manufacture in which these parts are assembled is called the caulking process [3].

The ball joint is made of a socket, bearing, plug, and ball stud. The plug prevents the components from being separated during manufacture and operation of the ball joint. The bearing, which has relatively much less stiffness among the components of the ball joint, serves as lubrication and buffering. The socket serves as the body of the temporarily assembled ball joint and plays a vital role in covering the internal parts with the plug through plastic deformation. The ball stud, which induces rotation in all directions is made by assembling the upper ball and bearing [2]. Hence, the science of tribology (friction, wear and lubrication) is highly required in the design and manufacturing of a ball joint, as in-depth understanding of this aspect can help reduce the effects of contacting surfaces and interplay of forces between these components. For the bearing, lubrication is required to reduce the rate of wear and as well improve the durability and life expectancy of the ball and socket joint. However, certain properties are considered while choosing lubricants for a vehicle ball joint, and this includes viscosity index (how lubricant viscosity changes with low and high temperatures), thermal stability, compatibility with the working environment, material, and characteristic of contacting surfaces, etc. Lubrication plays a vital role in the service performance of automobile ball joints, as insufficient lubrication tend to cause fretting and even squeaking [10, 11].

In Nigeria, the estimated road network as at 2016 is about 194,000 kilometers, and approximately 19% of these roads are paved, while 13% are unpaved with deteriorating conditions in terms of pot holes, poor drainage, etc. Both the paved and the unpaved roads in Nigeria are deteriorating by the day and have posed serious problems to vehicle users. A survey carried out on a total of 703 respondents showed that about 51% had their vehicles damaged in a month due to bad roads in their locality. Taking this to a national scale, about 51% of vehicle owners will encounter on or more vehicle problems in a month [12].

The rough surface road profiles in Nigeria has a significant influence on vehicles, causing unwanted vibrations on vehicle suspension systems due to kinematic excitations. In a moving vehicle, resonance vibration, frequencies imposed on the suspension system, quality of the road, velocity and acceleration of vehicles are some of the inevitable factors that exposes the suspension system and its surrounding component such as the ball joint to early fatigue and unforeseen failure. These phenomena are destructive, incurs expenses and require time to put the vehicle back in order.

The suspension system is affected as a result of these vibrations which in the long run may also increase the rate of stress distributions around the ball joint which is one of the most important component in a vehicle suspension system. The aforementioned forces, frequencies and fatigues which are imposed on the suspension system are transmitted to the ball joint. These factors reduce performance and longevity of the ball joint in service condition. For example, several vehicles are observed to have broken down on daily basis in Nigerian roads due to ball joint failure in which the ball stud pulls out from its socket, thereby, endangering the lives of vehicle owners, passengers, pedestrians as well as damages to the vehicle chassis. Finite Element Analysis (FEA) was employed in this paper to model and emulate the service condition of a vehicle ball joint and possible failures that arises during vehicle operation.

1.1. Forced Vibration of a Vehicle Ball Joint

A mechanical system undergoing forced vibration is due to the initial conditions and an external force acting on it. The mathematical model is a linear non-homogeneous differential equation of the second order given by equation 1;

$$\ddot{x} + 2\varsigma\omega_n\dot{x} + \omega_n^2 x = f(t) \quad (1)$$

Where

$$\omega_n = \sqrt{\frac{k}{m}}; \qquad 2\varsigma\omega_n = \frac{c}{m}; \qquad f(t) = \frac{f_{es}(t)}{m} \quad (2)$$

The general solution of this mathematical model is a superposition of the general solution of the homogeneous equation x_g and the particular solution of the non-homogeneous equation x_p.

$$x = x_g + x_p \quad (3)$$

The general solution of the homogeneous equation for the underdamped system is given equation 4;

$$x_g = e^{-\varsigma\omega_n t}(C_s \sin\omega_d t + C_c \cos\omega_d t) = Ce^{-\varsigma\omega_n t}\sin(\omega_d t + \alpha) \quad (4)$$

To produce the particular solution of the non-homogeneous equation, we assume that the excitation can be approximated by a harmonic function. Such a case is referred to as the harmonic excitation.

$$f(t) = q\sin\omega t \quad (5)$$

In the above equation, q represents the amplitude of the unit excitation and ω is the excitation frequency. Introduction of equation (1) into (5) yields;

$$\ddot{x} + 2\varsigma\omega_n\dot{x} + \omega_n^2 x = q\sin\omega t \quad (6)$$

In this case it is easy to predict the mode of the particular solution;

$$x_p = A_s \sin \omega t + A_c \cos \omega t \quad (7)$$

where A_s and A_c are constant. The function in equation 7 is the particular solution if and only if it fulfils equation (6) for any instant of time. Therefore, implementing it in equation 6 will give;

$$\left((\omega_n^2 - \omega^2)A_S - 2\varsigma\omega_n\omega A_c\right)\sin \omega t + (2\varsigma\omega_n\omega A_s + (\omega_n^2 - \omega^2)A_c)\cos \omega t = q \sin \omega t \quad (8)$$

This relationship is fulfilled for any instant of time if;

$$(\omega_n^2 - \omega^2)A_s - 2\varsigma\omega_n\omega A_c = q$$
$$2\varsigma\omega_n\omega A_s + (\omega_n^2 - \omega^2)A_c = 0 \quad (9)$$

Solution to the above equation yields the expression for the constant A_s and A_c in equation 10 and 11 respectively.

$$A_s = \frac{\begin{vmatrix} q & -2\varsigma\omega_n\omega \\ 0 & (\omega_n^2-\omega^2) \end{vmatrix}}{\begin{vmatrix} (\omega_n^2-\omega^2) & -2\varsigma\omega_n\omega \\ 2\varsigma\omega_n & (\omega_n^2-\omega^2) \end{vmatrix}} = \frac{(\omega_n^2-\omega^2)q}{(\omega_n^2-\omega^2)^2+4(\varsigma\omega_n)^2\omega^2} \quad (10)$$

$$A_c = \frac{\begin{vmatrix} (\omega_n^2-\omega^2) & q \\ 2\varsigma\omega_n\omega & 0 \end{vmatrix}}{\begin{vmatrix} (\omega_n^2-\omega^2) & -2\varsigma\omega_n\omega \\ 2\varsigma\omega_n\omega & (\omega_n^2-\omega^2) \end{vmatrix}} = \frac{-2(\varsigma\omega_n)\omega q}{(\omega_n^2-\omega^2)^2+4(\varsigma\omega_n)^2\omega^2} \quad (11)$$

Introduction of the expression in equation 9into the predicted solution in equation 7 yields

$$x_p = A_s \sin \omega t + A_c \cos \omega t = A \sin(\omega t + \varphi) \quad (12)$$

Where,

$$A = \sqrt{A_s^2 + A_c^2} = \frac{q}{\sqrt{(\omega_n^2-\omega^2)^2+4(\varsigma\omega_n)^2\omega^2}} \qquad \varphi = \tan^{-1}\frac{A_c}{A_s} = -\tan^{-1}\frac{2(\varsigma\omega_n)\omega}{\omega_n^2-\omega^2} \quad (13)$$

Or

$$A = \frac{\frac{q}{\omega_n^2}}{\sqrt{\left(1-\left(\frac{\omega}{\omega_n}\right)^2\right)^2+4\varsigma^2\left(\frac{\omega}{\omega_n}\right)^2}} \quad \varphi = -\tan^{-1}\frac{2\varsigma\frac{\omega}{\omega_n}}{1-\left(\frac{\omega}{\omega_n}\right)^2} \quad (14)$$

Introducing equation 4 and 12 into 3, the general solution of the equation of motion (6) can be obtained in the following form;

$$x = Ce^{-\varsigma\omega_n t}\sin(\omega_d t + \alpha) + A \sin(\omega t + \varphi) \quad (15)$$

The constants C and α should be chosen to fulfill the required initial conditions. For the following initial conditions;

$$x\,|_{t=0} = x_0 \qquad \dot{x}\,|_{t=0} = v_0 \quad (16)$$

The following set of the algebraic equations for determination of the parameters C and α can be obtained as;

$$x_0 = C_o \sin \alpha_o + A \sin \varphi \quad (17)$$
$$v_0 = -C_o\varsigma\omega_n \sin \alpha_o + C_o\omega_d \cos \alpha_o + A\omega \cos \varphi \quad (18)$$

Introduction of the solution into the general equations 18 (C_o, α_o) to the general solution, yields particular solution of the non-homogeneous equation that represents the forced vibration of the system considered [13];

$$x = C_o e^{-\varsigma\omega_n t}\sin(\omega_d t + \alpha_o) + A \sin(\omega t + \varphi) \quad (19)$$

Vibration of a Damped System is classified as the underdamped system, overdamped and the crically damped system which a typical vehicle ball joint in severe road conditions is subjected to. In this paper, the theory of any given ball joint under critically damped vibration is given as follows;

In critically damped vibration, the characteristic equation has two real and equal roots given by equation 20.

$$\lambda_{1,2} = -\varsigma\omega_n \quad (20)$$

The particular solutions are;

$$x_1 = e^{-\varsigma\omega_n t} \quad \text{and} \quad x_2 = te^{-\varsigma\omega_n t} \quad (21)$$

And their linear combination is

$$x = C_s e^{-\varsigma\omega_n t} + C_c te^{-\varsigma\omega_n t} \quad (22)$$

For the following initial conditions

$$x\,|_{t=0} = x_0 \qquad \dot{x}\,|_{t=0} = v_0 \quad (23)$$

The two constants C_s *and* C_c are as follow

$$C_s = x_0$$
$$C_c = v_0 + x_0\omega_n \quad (24)$$

Introduction of equations 22 and 24 produces an expression for free motion in the following form

$$x = e^{-\varsigma\omega_n t}\left(x_0 + t(v_0 + x_0\omega_n)\right) \quad (25)$$

$\omega_n = 1[1/s]$, $x_0 = 1[m]$, $v_0 1[m/s]$ and $\varsigma = 1$.

The critical damping offers the fastest way for a mechanical system to its equilibrium position.

2. Materials and Method

Primary data showing the dimensions of speedbumps within the University of Benin (UNIBEN) main Campus in terms of width and height as well as the depth of potholes were collected using measuring tape. The areas in UNIBEN main Campus where these measurements were taken includes Faculty of Engineering, auditorium, NDDC hostel, hostel clusters, medical complex, law, education, St. Albert and bank road as presented in Table1. The analysis was done using SOLIDWORKS static analysis and the conditions of the ball joint were simulated subject to the conditions of the road profile gotten from UNIBEN road profile above. The changes in height and depth were considered as excitation on a constant loading condition.

Table 1: Data Collected on University of Benin Road Profile

Location	Pothole (mm)	Speed bump	
		Height (mm)	Width (mm)
Faculty of Engineering	72	132	540
	56	119	870
	58	131	600
	43	83	660
Auditorium to NDDC hostel	85	108	570
	56	40	600
	97	87	880
	57	91	84
Hostel clusters	98	112	975
	84	101	440
	86	72	540
	79	86	600
NDDC to medical complex	82	64	460
	87	50	545
Medical complex to law	80	78	880
	67	73	635
Hostel clusters to education	97	60	420
	83	73	460
Auditorium to St. Albert	88	83	650
	85		
Education	62	65	900
	85		
Education to bank road	62	65	900
	63	86	980
	67	70	690
	73	73	760

3. Modelling of a Vehicle Ball Joint

The ball joint was modelled, taking into consideration the right material selection as used in real life application. Four new pieces of ball joints were acquired in the open market for Mercedes Benz C class 2010, Toyota Camry Sedan 2011, Honda Cross Tour 2010, Nissan Sedan 2011;and dimensions were measured for the ball, ball stud, socket internal and external diameter. As shown in Table 2, average dimension for each measured parts were used to model the ball joint in this paper.

Table 2: Average dimension for each measured parts

Parts	Dimensions(mm)
Ball	14.5
Ball Stud	6.5
Socket Internal Diameter	14.5
Socket External Diameter	2.10

where The dimensions were gotten from a new vehicle ball joint from the open market the actual ball joint and ensuring it had the three degrees of freedom using the software SOLIDWORKS. Secondly, the simulation was carried with the same software using data gotten from the measurement of speedbumps and potholes with the intention of subjecting it to our local road forces.Figure 1 represents CAD Model of the Ball Joint Developed with SOLIDWORKS while the Model Information andMaterial Properties are presented in Table 3.

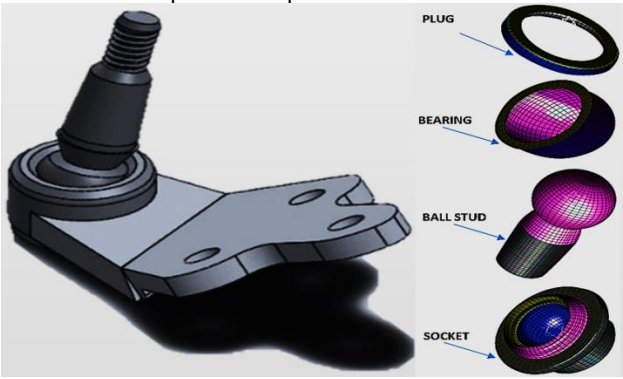

Figure 1: CAD Model of the Ball Joint Developed with SOLIDWORKS

Table 3: Model Information and Material Properties

Material Name	Alloy Steel	Mesh type	Solid Mesh
Model type	Linear Elastic Isotropic	Mesher Used	Blended curvature-based mesh
Default failure criterion	Max von Mises Stress	Jacobian points	4 Points
Yield strength	6.20422e+08 N/m^2	Maximum element size	9.40316 mm
Tensile strength	7.23826e+08 N/m^2	Minimum element size	2.1089 mm
Elastic modulus	2.1e+11 N/m^2	Total Nodes	23455
Poisson's ratio	0.28	Total Elements	14682
Mass density	7700 kg/m^3	Maximum Aspect Ratio	38.903
Shear modulus	7.9e+10 N/m^2	% of elements with Aspect Ratio < 3	92.7
Thermal expansion coefficient	1.3e-05 /Kelvin	% of elements with Aspect Ratio > 10	0.395

4. Results and Discussions

In Finite Element Analysis, mesh sizes with low aspect ratio is a good tool for determining margins of safety, since it can closely predict the maximum stress levels. However, selecting a high value for the minimum element size mesh control may result in the generation of solid elements with high aspect ratio by the mesh generator.Most Finite Element tools provide meshing that generate adequate element, but none of them provides the room for automatic mesh selection and control. As shown in Figure 2, curvature based mesh was employed and the maximum aspect ratio of 38.903 was obtained. To increase the performance of the finite element performance, map meshing (mesh controller) was employed to control the aspect ratio of the element in order to produce a consistent mesh. According to Picasso [14], other advanced methods such as adaptive meshing can also be employed to estimate the errors and eliminate meshes with high aspect ratio. Figure 3 shows the frequency curve obtained from Uniben road profile.

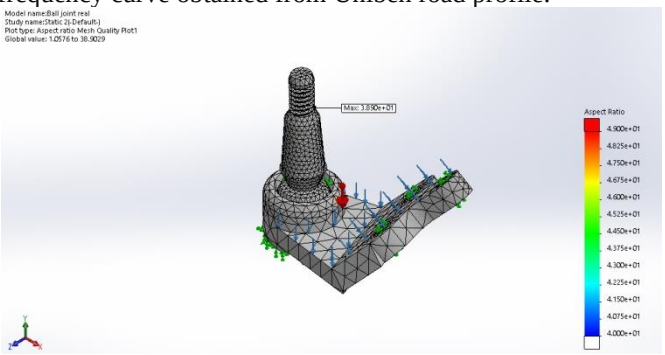

Figure 2: Mesh Quality Plot for the Ball Joint Model

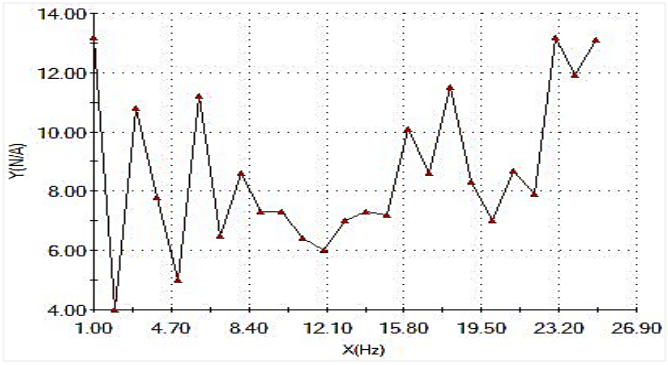

Figure 3: Frequency Curve obtained from the Uniben road profile

Since it is impractical to test every material and the combination of their stresses (σ_1, σ_2 and σ_3), it may be essential to employ finite element methods for examining the tribology of moving parts and for predicting possible failures based on the material and component performance in service condition. Failure in ductile materials like AISI 45566 ball joint material in this paper is due to relative sliding of material atoms within their lattice structure, as a result of shear stresses accompanied by distortion of the components shape. Every material possesses a definite limited capacity (elastic limit) to absorb distortion energy, during which the material yields or fails when this capacity is exceeded. This is in agreement with von mises yield criterion (also known as the maximum distortion energy criterion) which states that yielding of a ductile material begins when the second deviatoric stress invariant reaches a critical value[15, 16]. As shown in the static and dynamic analysis in Figure 4 and 5,maximum von mises stresses of 377 N/mm^2 and 454 N/mm^2 were obtained for both analysis were below the yield strength of the material (620 N/mm^2), indicating that a given ball joint operating under this is safe except the material yield strength is exceeded by its von mises stress. At this point, the material stops being elastic and becomes plastic.

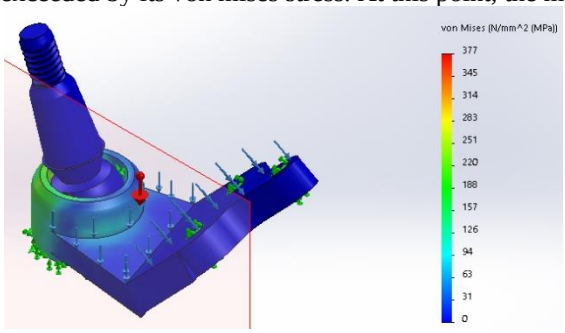

Figure 4: Von-mises Stress values obtained from the static analysis

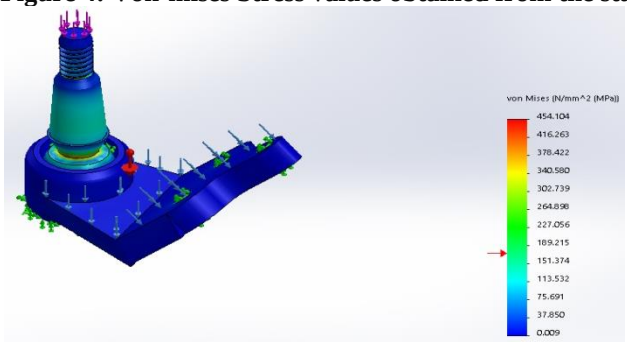

Figure 5: Von-mises Stress values obtained from the Dynamic analysis

The Factor of Safety (FOS) is defined by the ratio of the Design load to the von-mises stress. In engineering applications, FOS must be kept as high as possible although the design of a given component with very higher FOS may be considered to be too expensive despite its high strength and longevity. In this study, FOS was selected on a scale of 1-10 and the values obtained for different components of the ball joint are shown in the distribution chart in Figure 6 while Figure 7 shows the graphical representation of Dynamic Response due to Load on the Ball Joint. Figure 8 is the fatigue analysis of the ball joint model while Figure 9 represents the total life predicted for the Ball Joint Model in Years.

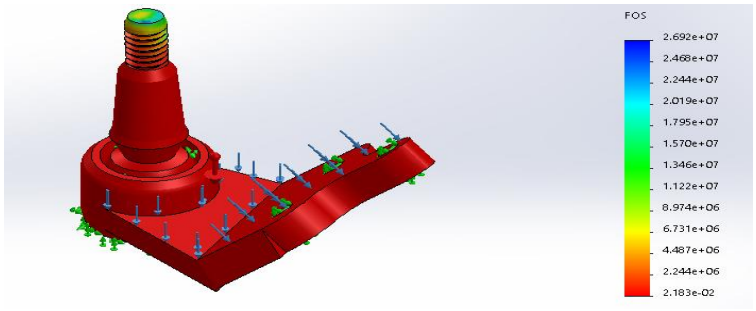

Figure 6: Factor of Safety (FOS) for the Ball Joint Model

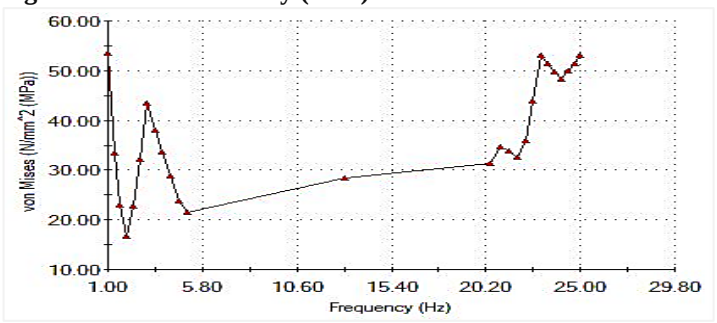

Figure 7: Graphical Representation of Dynamic Response due to Load on the Ball Joint

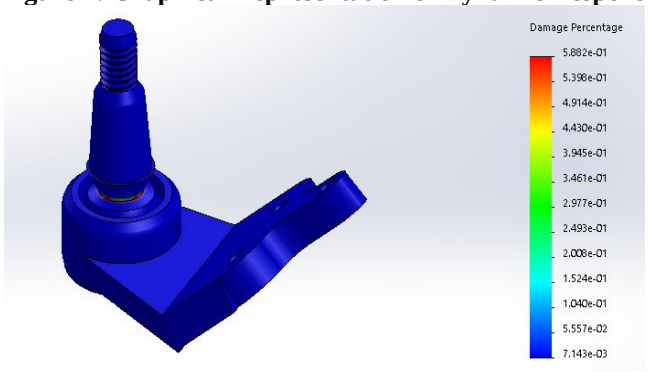

Figure 8: Fatigue Analysis of the Ball Joint Model in Service Condition

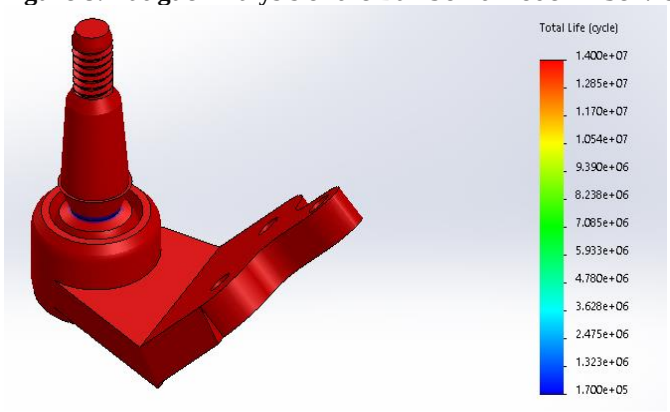

Figure 9: Total Life Predicted for the Ball Joint Model in Years

As shown in Figure 8, fatigue analysis helps identify how repetitive load cycles cause structural failures. This load cycles are the same as those used in the dynamic study. This helps identify failure in components subjected to stresses less than its yield and do not experience plastic deformation and have relatively long lives. Calculations of fatigue requires an S-N curve in addition to loading data. This curve is gotten from material property.

From the fatigue analysis carried out, it can be said that the material minimum fatigue life as a result of varying loading is 170000 cycles

And given the average distance between bumps to be 10m and the speed of bump approach to be 9km/h (2.5m/s). The frequency becomes 0.25Hz.

From this frequency it is seen that the time taken for fatigue failure will be the cycle divided by the frequency. T=680,000sec. Assuming drivers drivea vehicle at an averageof 1 hour per day (3600 sec), the ball joint may likely fail after 189 days, which is approximately 6 months.

From the results obtained from the analysis, it was observed that various factors affect the service life of the ball joint having the major factor to be bad roads, in addition to the information on weather being a factor that affects the ball joint, some of the mechanics made it clear by stating that it was the stagnant water from the potholes in which these ball joints were continually submerged in that is actually harmful to the component. In addition, this harmful effects can increasewhen the ball joints are constantly exposed to rain water particularly when the joints are not protected by their rubber boots.

5. Conclusion

Comparing the failure period of the ball joint from the FEA and statistical analysis, we see a close similarity in the failure period but the slight difference may be due to inability of the software to accurately depict the bad road conditions and other factors responsible for the ball joint failure. Other factors may be due to the reducedtimeframe in which the statistical data was acquired. This study has clearly indicated that the failure of a ball joint during service operation can be prevented if it is modelled and simulated by manufacturers before installation in vehicles. This is because, the simulation process which identify the areas that are prone to unwanted defects and failure reveals the severity of defects on the component for manufacturers to improve on. Thus, the longevity of vehicle ball joints can be prolonged for optimum performance, minimal failure, significant reduction in road accident and vehicle breakdown which is a major cause of traffic gridlocks in highways.

References

[1] Brown, S., and Clarke, I. (2006), A Review of Lubrication Conditions for Wear Simulation in Artificial Hip Replacements, Tribology Transactions, 49, 72-78.

[2] Sin, B.U and Lee, K.H (2014) Process Design of a Ball Joint, Considering Caulking and Pull-Out Strength. Dong-A University, Republic of Korea.

[3] Kim, S. (2015) Method for Manufacturing Ball Joint, Patent, Central Cooperation, United states No: US9011744B2.

[4] Shinde, J., Kadam, S., Patil, A. and Pandit, S. (2016) Design Modification and Analysis of Suspension Ball Joint Using Finite Element Analysis, Journal of Innovative Research in Science, Engineering and Technology, 5(7), 12797-12804.

[5] Shinde, J. and Kadam, S. (2016) Design of Suspension Ball Joint Using FEA and Experimental Method, International Research Journal of Engineering and Technology, 3(7), 1853-1858.

[6] Christensson, J. and Halldorf, J.(2017) Library of Bushings and Ball Joints in CAD Environment. Chalmers University of Technology, Gothenburg, Sweden.

[7] Baerlocher, P. and Boulic, R., (2001) Parametrization and Range of Motion of the Ball and Socket Joint, Swiss Federal Institute of Technology, 1015 Lausanne, Switzerland.

[8] Raes, S., Devreese, T., De Pauw, J. and De Beaets, P., (2015) Design of A Tribological Ball Joint Tester, 6(1), 1-5.

[9] Valentini, P. P. (2013) Effects of the Dimensional and Geometrical Tolerances on the Kinematic and Dynamic Performance of the Rzeppa Ball Joint. Proceedings of the Institution of Mechanical Engineers, Part D: Journal of Automobile Engineers, 0(0), 1-13.

[10] Kang, K. (2015) Theoretical Model for Friction-Induced Vibration of Ball Joint System under Mode-Coupling Instability. Tribology Transactions, 58(5), 807-814.

[11] Bordon, W., Zucchini, M., Simiao, G. and Cichoski, B W. (2003) High Performance Ball Joint. Society of Automotive Engineers 000000223PE.

[12] Enwerem, G. C. and Ali, G. A., (2016) Economic Effects of Bad Roads on Vehicle Maintenance in Nigeria, International Journal of Scientific and Research Publications, 6(6), 761-766.

[13] Krodkiewski, J. M. (2008) Mechanical vibration, 436-431 Mechanics 4, Unit 2, The University of Melbourne.

[14] Picasso, M. (2006) Adaptive Finite Element with Large Aspect Ratio Based on an Anisotropic Error Estimator involving first Order Derivatives. Computer Methods in Applied Mechanics and Engineering, 196(1-3), 14-23.

[15] Ikpe, A. E., Owunna, I. B. and Satope, P. (2017)Design optimization of a B-pillar for crashworthiness of vehicle side impact. Journal of Mechanical Engineering and Sciences, 11(2), 2693-2710.

[16] Ikpe, A. E. and Owunna, I. (2017) Design of Vehicle Compression Springs for Optimum Performance in their Service Condition, International Journal of Engineering Research in Africa, 33, 22-34.